


Please cite the Published Version

Haider, Daniyal, Ren, Aifeng, Fan, Dou, Zhao, Nan, Yang, Xiaodong, Tanoli, Shujaat Ali Khan, Zhang, Zhiya, Hu, Fangming, Shah, Syed Aziz  and Abbasi, Qammer H (2018) Utilizing a 5G spectrum for health care to detect the tremors and breathing activity for multiple sclerosis. Transactions on Emerging Telecommunications Technologies, 29 (10). e3454. ISSN 2161-3915

DOI: <https://doi.org/10.1002/ett.3454>

Publisher: Wiley

Version: Accepted Version

Downloaded from: <https://e-space.mmu.ac.uk/624428/>

Additional Information: This is the peer reviewed version of the article which has been published in final form at 10.1002/ett.3454. This article may be used for non-commercial purposes in accordance with Wiley Terms and Conditions for Self-Archiving.

Enquiries:

If you have questions about this document, contact openresearch@mmu.ac.uk. Please include the URL of the record in e-space. If you believe that your, or a third party's rights have been compromised through this document please see our Take Down policy (available from <https://www.mmu.ac.uk/library/using-the-library/policies-and-guidelines>)

Utilizing 5G Spectrum for healthcare to detect the tremors and breathing activity for Multiple Sclerosis.

Daniyal Haider, Aifeng Ren, Dou Fan, Nan Zhao, Xiaodong Yang, Shujaat Ali Khan Tanoli, Zhiya Zhang, Fangming Hu, Syed Aziz Shah, Qammer H. Abbasi

Abstract—Utilizing 5G sensing in the health care sector with increased capacity and massive spectrum range increases the quality of health care monitoring system. In this paper 5G C-band sensing operating at 4.8GHz is used to monitor particular body motion of Multiple Sclerosis patient especially the tremors and breathing pattern. The breathing pattern obtained using 5G C-band technology is compared with invasive breathing sensor to monitor the subtle chest movements caused due to respiration. The 5G C-Band has huge spectrum from 1 GHz to 100GHz, which enhances the capacity and performance of wireless communication by increasing the data rate from 20Gbps to 1Tbps. The system captures and monitors the wireless channel information (WCI) of different body motions and efficiently identifies the tremors experienced since each body motion induces a unique imprint that is used for particular purpose. Different machine learning algorithms such as support vector machine (SVM), K-nearest neighbor (KNN), and random forest (RF) are used to classify the WCI data obtained for various human activities. The values obtained using different machine learning algorithms for various performance metrics such as accuracy, precision, recall, specific, Kappa and F-measure indicate that the proposed method can efficiently identify the particular conditions experienced by multiple sclerosis patients.

Index Terms— Multiple Sclerosis (MS), Wireless Channel Information (WCI), Support vector machine (SVM), K-Nearest Neighbor (KNN), Random Forest (RF), C-band sensing, and 5G spectrum.

1. INTRODUCTION

The health-care industry is focusing on increasing the standards of health and diagnosis by emphasizing on wireless sensor networks. Wireless sensing is improving the quality of life by providing efficient sensing of the symptoms [1]. C-band sensing operating at 4.8GHz frequency becoming increasingly important by utilizing 5G spectrum [2-3]. There is globally a development going on in wireless networks and communication and has made easy for users to send and receive the

Daniyal Haider and Syed Aziz Shah are with the School of International Education, Xidian University, Xi'an, Shaanxi, China, 710071

Aifeng Ren, Duo Fan, Nan Zhao, Xiaodong Yang, Zhiya Zhang, Fangming Hu are with the School Of Electronics Engineering, Xidian University, Xi'an, Shaanxi, China, 710071.

Shujaat Ali Khan Tanoli is with the Department of Electrical Engineering, COMSATS University, Attock, Pakistan.

Qammer H. Abbasi is with the School of Engineering, University of Glasgow, Glasgow G 12 8QQ, UK.

Corresponding author: Xiaodong Yang

Email: xdyang@xidian.edu.cn

The work was supported in part by the Fundamental Research Funds for the Central Universities (JB180205), National Natural Science Foundation of China (61671349, 61301175, 61601338), International Scientific and Technological Cooperation and Exchange Projects in Shaanxi Province (Grant No 2017KW-005).

information safely and easily from one point to another point at any time [4]. This modern era of media development, where everything is digitalizing is changing the health-care sector and has many features like digitalization of many health-care products and also including personalization and fragmentation. Through the media development many persons getting knowledge about modern health-care sector and how to solve the health related issues by using the technology. This encourages people to discuss the development and spread the education about the modern health-care sector.

Wireless communication is providing reliable and safe multiple users environment and with inclination towards 5G, quality of wireless communication and sensing is increasing rapidly. Many applications which require high data are now applicable in 5G by providing adequate and safe network with optimized transmitted traffic utilizing the affective spectrum. This also includes the machine-type communication (MTC) and communication involving low latencies. Applications related to MTC are very important in 5G communication which includes stationing of many linked devices to perform operations like surveillance and monitoring of many objects [5]. Conclusively applications involving human-to-machine interaction are going to be revolutionary in health-care sector and C-band sensing is making this easy by using 5G by providing reliable and low latency sensing scenarios [6]. In 5G the effective spectrum utilization makes it feasible for all of the wireless communication and support the massive amount of wireless connections due to increase in capacity.

5G is emerging strongly in the society by aiming to create or develop the hyper connected society by utilizing the licensed and unlicensed spectrum for wireless technology and IoT technologies. Researchers are focusing on the improvement of spectral utilization rather than spectral efficiency. It will be helpful for the wireless networks to become more flexible and allocate the resources for diverse connections. The key features supported by 5G technology includes high data rate usage and affective spectrum utilization for different application like VR, secure and reliable communication for mobile health care and many other sensitive wireless networks and huge machine type communication to support massive IoT.

Wireless sensing is improving the life and also the health sector by monitoring patients and their body motion at hospital to reduce the adverse effects of diseases. Multiple sclerosis (MS) is motion related and neurodegenerative diseases which needs to be diagnose to maintain the healthy life. This disease is related to the mobility impairment in which nervous system of a person is directly affected and causes many functional disabilities with the passage of time. Millions of people are affected by this disease [7], which could be addresses as chronic progressive neurological disorder and shows bad effects by decreasing quality of life. MS is demyelinating disease of a central nervous system [8] which consists of brain, spinal cord and optic nerve. Multiple Sclerosis affects the person from ages 20 – 40 years old and symptoms related to bouts can typically worsens and can linger for months without treatment. One common tree of MS symptoms is called Charcot's neurologic triad that includes dysarthria which is difficult or unclear speech and difficult to eat and talk, nystagmus which is involuntary eye movement affecting the vision and making the vision blurry or double and the most dangerous is the intention tremors. These intentional tremors are very dangerous which includes muscle weakness, spasms, tremors and ataxia (loss of balance). In serious cases this leads to paralysis.

MS affects the higher order activities to the brain causing poor concentration and critical thinking and also the depression and anxiety. It also affects the respiratory system of human due to weak respiratory muscles [9-11]. In this patient lose control over breathing which may lead to respiratory arrest and sleep apnea. The research also proved that patients with swear MS has greater chance of Obstructive sleep apnea (OSA) and central sleep apnea (21%) [12].

The MS patient needs deep attention and affective monitoring scenario in order to control the tremors. This paper presents monitoring of particular conditions such as tremors and breathing pattern using C-Band 5G sensing which has greater impact in health-care sector. We also observed the biomarkers such as, sitting, lying, falling and tremors along breathing pattern. We used three algorithms for the classification of data. The SVM, KNN and RF algorithms.

The organization of the paper is as follow, Section 2 cites the related work on MS. Section 3 presents the overview of 5G wireless communication. Section 4 presents the core idea of SVM, KNN and RF algorithm. Section 5 cites the proposed solution. Section 6 cites the result and its discussion and Section 7 explains the final conclusion. The overall symbols used in the paper are mentioned in Table 1.

Table 1: Symbols used in the paper.

Symbols	Abbreviations	Symbols	Abbreviations
MS	Multiple Sclerosis	IoT	internet Of Thing
WCI	Wireless Channel Information	LOS	Line-Of-sight
SVM	Support Vector Machine	NLOS	Non-Line-Of-sight
KNN	K-Nearest Neighbor	NIC	Network Interface Card
RF	Random Forest	CFR	Channel Frequency Response
OSA	Obstructive sleep apnea	AP	Access Point
FES	Functional Electrical stimulation	Tp	True Positive
ILC	Iterative learning Control	Tn	True Negative
D2D	Device-To-Device	Fp	False Positive
TDD	Time Division duplex	Fn	False Negative
SMO	Sequential Minimal Optimization		
MTC	Machine Type Communication		

2. RELATED WORK

Recently, many approaches are being implemented to monitor the patient with Multiple Sclerosis. None of the work or technique monitors the different body postures during MS relapses. Barry R. Greene et al. [13] presented the idea of examining the patient's mobility with the help of shank mounted inertial sensors. This study was conducted to distinguish the healthy patient from MS patient. Jiaqi Gong et al. [14] also presented the idea of utilizing the inertial body sensors to observe the mobility of a patient. In this idea causality analysis method was used where subjects performed 6MW test by wearing inertial body sensors. Patrica Sampson et al. [15] presented the usage of Functional Electrical stimulation (FES) with passive robotic support while performing virtual reality tasks for the improvement of upper limb function of patient with MS. According to that proposed idea, patients with MS were assisted to walk on the specified trajectory path for six times together with the employment of iterative learning control model (ILC). Regression analysis was used to analyze the accuracy of training analysis with and without FES. This work showed the feasibility of using FES along with passive robotic assistance for the improvement of arm movement and control in MS. Dimitris Kastaniotis et al. [16] presented the work in which the state of a MS patient was assessed by video-based system. This system was used to analyze and capture the gait sequence from two minute walk test performed by MS patient. This technique made possible of differentiating the healthy patient from MS patient. Fei Yu

et al. [17] presented the idea by using the portable wireless medical sensor devices for studying fatigue in MS patients. With the help of the wireless devices capturing of Electrocardiogram, eye movement detection and body skin temperature detection was performed.

All of the above mentioned approaches are useful for diagnosing MS but none of the approaches present the clear picture or procedure to analyze different body postures of an MS patient, which includes tremors, seizures, jerky body movement and also the abnormalities in breathing pattern. Living with MS without proper monitoring of the symptoms is unhealthy and also affects the life of family members. Monitoring the symptoms on time for proper diagnosis is utmost importance. This disease has adverse effect on a person's life and one must have proper care and attention to overcome the symptoms that appears with the passage of time.

Our approach focuses on the monitoring of different body movement [23] and breathing pattern during MS. In this research we use 5G sensing by utilizing the affective spectrum with range of 4.8 GHz frequency [2-3] to get the wireless channel information for different body gestures by utilizing wireless devices [21]. Various machine learning algorithms such as (SVM) [19, 20], KNN, and RF are used for the classification of data acquired using small wireless devices operating at C-Band. In this way we are able to provide timely attendance by knowing the current condition and body movement of MS patient. We also monitored the breathing activity [25] of MS patient with invasive breathing sensor and compared it with WCI of breathing from C-band sensing. We also used Spearman rank correlation for the comparison of breathing signal from C-Band and digital respiratory sensor.

3. 5G WIRELESS COMMUNICATION

Precision and reliability is an important factor in 5G wireless communication. In healthcare sector leveraging wireless devices for monitoring purposes, reliable environment to observe the output from the system for the correct observation of any motion related disease symptoms must be provided. The proposed method uses the wireless devices such as network interface card, Omni-directional antenna and an access point operating at 4.8 GHz, which allows 30 subcarriers to reveal the channel measurement in the form of wireless channel information (WCI) to the user [22]. The received signal can be represented as:

$$y = hx + n \quad (1)$$

Where y is the received signal, h is the channel information (fading coefficient if channel is fading channel), x is the transmitted signal and n is the white Gaussian noise with means equals to 0 and variance equals to σ^2 .

The value of h could be a fading coefficient if the channel conditions includes deep fading so its representation is as follow,

$$h = \sum_{i=0}^{L-1} a_i e^{-j2\pi f_c \tau_i} \quad (2)$$

This h is the sum of multiple signal components and can be represented as,

$$h = \sum_{i=0}^{L-1} a_i \cos 2\pi f_c \tau_i - j \sum_{i=0}^{L-1} a_i \sin 2\pi f_c \tau_i \quad (3)$$

Here a_i is the attenuation and τ_i indicates the delays for the multiple signal components and are random in nature. This represents the Gaussian nature of the signal components.

The h holds all the information about the channel and information about the possible multipath signal components. The wireless devices give the WCI, which holds all the information about amplitude and phase for all the subcarriers unlike the RSSI, which only gives the information about amplitude of the signal. The RSSI could not characterize the multipath propagation so in case of breathing detection it may produces the false breathing patterns. In this model we measure the refined WCI to observe the body postures and breathing patterns as well.

The 5G wireless communication focuses on the speed, high data rate and reliability for the wireless communication and to support the futuristic usage of Internet of Things. The key goal of 5G is to globalize the pervasive connectivity for any device with any application at any time. As mentioned earlier the health sector is now focusing on the wireless solutions for the patient monitoring purpose and 5G is the core for that by providing reliable wireless communication anytime at any place.

In 5G, spectrum allocation is important and it provides the unified spectrum distribution. Like Sub GHz used for the massive IoT supporting long range, 1GHz to 6GHz to support the wider bandwidth for the eMBB and above 6GHz with mm wave for the extreme BW and the shorter range broad band. In 5G the spectrum division makes it possible to handle huge range of applications on a single wireless network including the Machine type applications. The licensed and unlicensed spectrums avoid the spectrum fragmentation in 5G and support full range of wireless technology. The timeline for the 5G is shown in Figure 1.

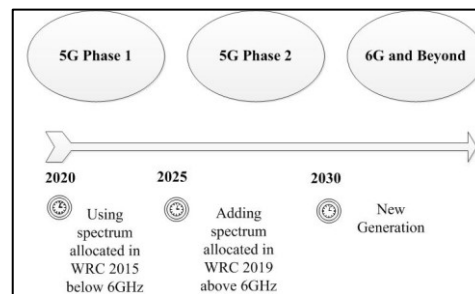


Figure 1: Time line for 5G.

There are some other technology components of 5G wireless access beside the operation at higher frequencies, which includes device-to-device communication, access/backhaul integration, Multi antenna transmission, flexible duplex, ultra-lean-design, and flexible spectrum usage and control separation [29].

5G will make it possible to use wireless link and the backhaul together with efficient utilization of the spectrum. The device-to-device communication will be considered as the starting part for the wireless access solution in the 5G era and also as the important part of wireless system. D2D could be effective for the offload traffic as well to reduce the interference in the wireless link. Frequency Division Duplex considered as the key part for the wireless communication and in the 5G for the lower frequencies this will be the important duplex scheme. Furthermore in 5G there will be flexible scenario for the usage of TDD.

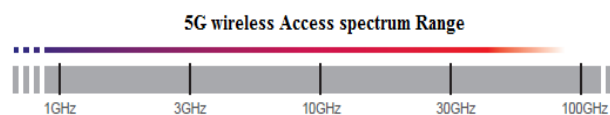


Figure 2: 5G Spectrum.

The overall 5G spectrum range is shown in Figure 2, so the main focus of the 5G technology is always revolve around the improvement or enhancement of the capacity and for this the effective utilization of licensed and unlicensed spectrum is necessary. The expected capacity of 5G will reach from 20Gbps to 1Tbps and researchers making it possible by considering high frequencies band. All this is very useful for the health sector as the capacity of the network increases, it will be possible to exchange more data related to patient health between different hospitals and research centers for the improvement of diseases and discovery of new diagnoses. In this research 5G plays very important role and will make it possible to enhance the mobile health sector in future.

4. DATA CLASSIFICATION APPROACHES

The categorization of data into their particular classes is known as the data classification process. Numerous techniques are available for the data classification which includes Support Vector Machine (SVM), Neural Networks (NN) [31], K- Mean, K-Nearest Neighbor (KNN) [30] and Random Forest (RF) [32] etc. In this paper we used SVM for the data classification and also compared the results with KNN and RF.

4.1 Support Vector Machine (SVM)

SVM is the supervised machine learning method that classifies given data into particular class [19]. The SVM classifier works on two or more classes and separates the classes from each other with the help of a hyperplane. The hyperplane is a simple decision boundary or a separation between two classes. The close points to the hyperplane, which helps in the construction, are known as support vectors. Thus this algorithm is called a support vector machine. The data for the classification is composed of data instances which are called the feature vectors [20]. If we consider two class problems C1 and C2 as shown in Figure 3, the general hyperplane can be represented as,

$$w^T p + w_o = 0 \quad (4)$$

Here w is the weight vector which is perpendicular to the hyperplane, p is the input feature vector and w_o is the bias function. If the dimensionality of the feature vector is more than 3 then the above linear equations represents the hyperplane. The graphical representation of two classes is shown in Figure 3, where two classes are being separated by the hyperplane.

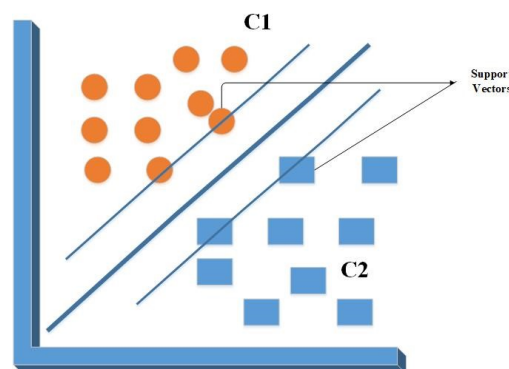


Figure 3: SVM feature space.

For every feature vector p , equation 4 must be computed and for positive side and negative side position of the feature vector x , we get,

$$\begin{aligned} w^t p + w_o &> 0 \Rightarrow \langle p \in C1 \rangle \\ w^t p + w_o &< 0 \Rightarrow \langle p \in C2 \rangle \end{aligned} \quad (5)$$

Considering class belongingness y_i to a vector p_i , where it is represented as $y_i = +1$ for class C1 and $y_i = -1$ for class C2. And hence we can get,

$$y_i (w \cdot p_i + w_o) > 0 \quad (6)$$

The margin of the hyperplane must be as maximum as possible,

$$\frac{w \cdot p + w_o}{\|w\|} \geq \gamma \quad (7)$$

So to get the optimal hyperplane, $\|w\|$ must need to be minimized and w_o to be maximized.

$$\min \Phi(w) = \frac{1}{2} w \cdot w \quad (8)$$

So we have the constraint under which $\|w\|$ will be minimized which is,

$$y_i (w \cdot p_i + w_o) = 1 \quad (9)$$

Lagrangian multiplier α_i will be used for the minimization process,

$$L(w, w_o) = \frac{1}{2} (w \cdot w) - \sum \alpha_i [y_i (w \cdot p_i + w_o) - 1] \quad (10)$$

After the derivation w.r.t to w and w_o , the final lagrangian expression will be,

$$L = \sum_{i=1}^m \alpha_i - \frac{1}{2} \sum \alpha_i \alpha_j y_i y_j (p_j \cdot p_i) \quad (11)$$

After the minimization process the final decision function is as follow,

$$F(p) = \text{sign} \left[\sum_{i=1}^M \alpha_{o,i} (p^t p_i) + w_o \right] \quad (12)$$

In Equation 12, p is the input vector for classification, M represents the support vectors and the $\alpha_{o,i}$ represents the support vectors among the given input vectors.

Moreover, the kernel functions support the phenomena of casting vectors from lower dimension to the higher dimension. Linear hyperplane with the mapping function $\varphi(\bar{p})$ will be used for the classification,

$$F(p) = \text{sign} \left[\sum_{i=1}^M \alpha_{o,i} (\varphi(p) \varphi(p_i)) + w_o \right] \quad (13)$$

Kernel function represents the dot product of the vector in upper dimension space and always overcome the numerical optimization. Finally by using this kernel function the decision rule represented as,

$$F(p) = \text{sign} \left[\sum_{i=1}^M \alpha_{o,i} K(p, p_i) + w_o \right] \quad (14)$$

Classification of the data totally depends upon the kernel functions and in this research we used polynomial, linear and radial basis function, etc. In high dimension other than 2D, these Kernel functions are always helpful and SVM classifies the data in correct order by using them. The proposed SVM procedure is shown in Figure 4.

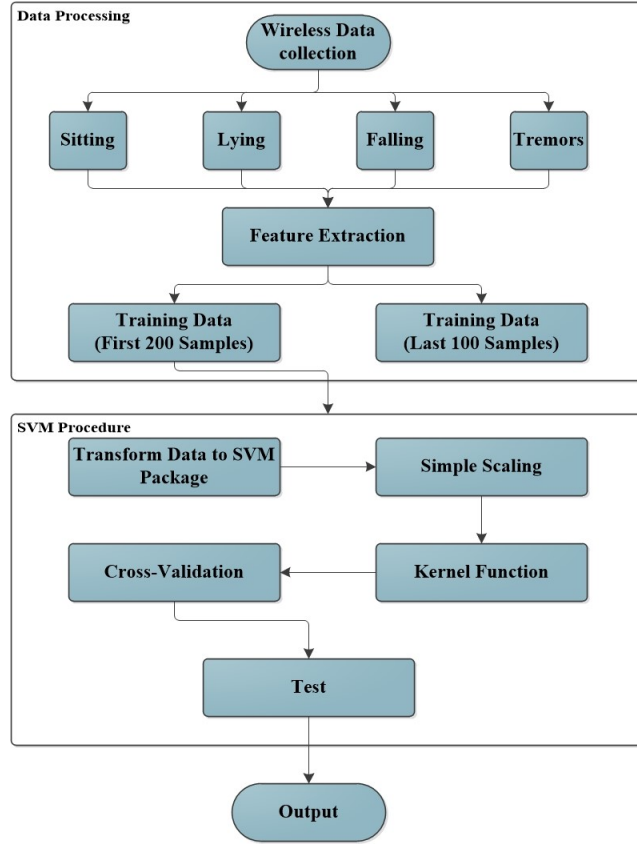


Figure 4: SVM Procedure's overview.

4.2 *K*-Nearest Neighbor (*K*-NN)

The KNNclassification method works simply by choosing the K nearest training samples in the given feature space. Theclassification of the dataset is performed by nearest neighbors following the majority vote. The common class in the K nearest neighbors is assigned with the dataset. For the distance function, if $K = 1$ means the nearest neighbor class contain the given dataset. There are three distance functions used in KNN algorithm and are represented as:

$$Manhattan = \sum_{i=1}^k |x_i - y_i| \quad (15)$$

$$Minkowski = \left(\sum_{i=1}^k |x_i - y_i|^q \right)^{1/q} \quad (16)$$

$$Euclidean = \sqrt{\sum_{i=1}^k (x_i - y_i)^2} \quad (17)$$

$$Hamming Distance = D_H = \sum_{i=1}^k |x_i - y_i| \quad (18)$$

Hamming distance function is used when the categorical variables are present. The value for k is chosen through careful consideration of the available dataset. Noise shows direct relation with the value of k , as noise reduces by increasing the value of k .

4.3 Random Forest (RF)

The random forest algorithm performs the classification by using the predictors and enhances the performance by reducing the overall computational cost. The regression tree is employed in the algorithm by the random selection features using the given data set. At every node split is identified with the help of available trees [33]. This algorithm introduces the parallel computing and the sub model for each of the subset without the communication with the CPU. This in short reduces the training samples.

5. PROPOSED DESIGN

The proposed methodology leverages C-band sensing operating at 4.8GHz over the wireless channel. The technique is used for the tracking of many body movements. Hence providing different wireless channel signatures that represent the wireless channel information. The small scaled wireless devices such as wireless transmitter operating at 4.8 GHz along with the network interface card mounted in a computer and an Omni-directional antenna is used to extract the wireless data of different body movements.

Wireless communication is deeply affected by the multipath fading. The communication between wireless transmitter and receiver hold many multipath signal components which occur due to the reflection, scattering or diffraction. We proposed the method where we detect the different body motions [23] like walking, lying, falling and tremors using the 5G C-band technique. The human body acts as an obstacle between signal paths as shown in Figure 5. The desired signal propagates through multiple paths and generates the multiple copies of the signal, which then received by the wireless receiver. The wireless channel information (WCI) [21] recovered from the NIC carries the information of 30 sub-carriers and the raw phase and amplitude information of the received sub-carriers. For the classification of the extracted WCI, we used support vector machine (SVM), K-NN and RF classifiers. We also evaluate the three classifiers by using the different performance matrices like accuracy, recall, specificity, precision, Kappa and F-measure.

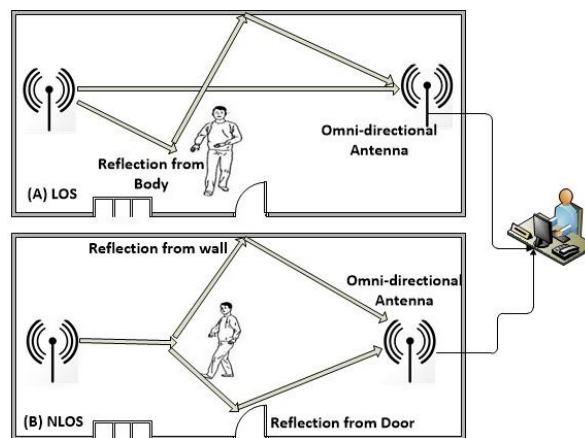


Figure 5: LOS & NLOS signal propagation during body movement.

We also monitored the human breathing activity [25] by utilizing the WCI from C-band. In MS the respiratory system of a person does not perform accordingly, so it is necessary to monitor the shortness of breath during sleep[10, 12]. This method is used to detect the normal and abnormal breathing of MS patient with the help of WCI extracted from C-Band and an invasive breathing sensor. We then compared the extracted data from both C-Band and digital respiratory sensor. We also monitored the minute chest movement from the extracted WCI. As mentioned earlier the signal from the transmitter to the receiver propagates in a straight line called LOS but if the signal experiences any obstacle the LOS changes in to NLOS propagation. In the breathing detection the continuous movement of chest while breathing shifts the signal from LOS to NLOS. So the WCI data will be different due to continuous chest movement. As shown in the Figure 6(a) a person lying on the bed in line-of-sight between the transmitter and receiver. As a person inhale and exhale, the continuous chest movement disturbs the line-of-sight signal and shows the unique signature in WCI. Also in the Figure 6(b) the multiple copies of the signal is received at the receiver side after reflected back from the walls.

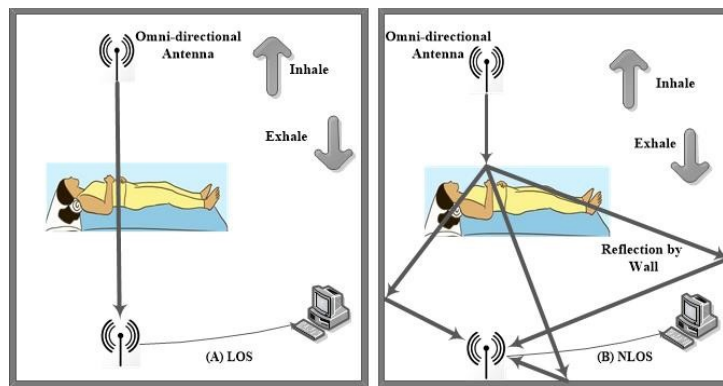


Figure 6: Breathing motion for LOS and NLOS path.

6. RESULTS & DISCUSSION

This portion explains how the 5G sensing is used and how it helps to improve the quality of life. The experiment was performed using very cheap wireless devices by keeping in mind the modern communication standards. A simple transmitter connected with RF generator (SMA 100B) acts as an access point (AP) and operates at the frequency of 4.8GHz. An advance HP desktop computer mounted with ASUS ACE 100 4 x 4 (ASUS PCE-AC88)dual band PCI, NIC card connected with Omni-directional antenna, act as a receiver and then connected to the AP. For the different posture detection a person imitates various body movements between the transmitter and the receiver for multiple times for the period of 2 minutes each. We took multiple numbers of measurements to extract the precise WCI for all the body motions. For the WCI extraction of body motion the average distance between the devices was adjusted between 4 to 5 meters and for breathing detection the distance adjusted between 1 to 1.5 meters.

6.1 Posture Detection

The body postures and breathing detection was performed as shown in Figure 5 and 6. The AP pings at the rate of 20 packets per seconds and data was collected at the client side. The client side was then upgraded with the updated drivers [22].The signal travels in LOS and NLOS and contains multiple copies of signal components.The transmitted data received by the transmitter

in the form of a matrix H . This matrix H is known as channel frequency response (CFR) of size 30×1 . The rows and columns represent the significant entities, like frequency represented by number of rows and receiving antennas represented by the columns. If we consider the n^{th} received packet CFR,

$$CFR_n = [h^1(n), h^2(n), h^3(n), \dots, h^{30}(n)] \quad (19)$$

Where $h^i(n)$ represent the CFR for the subcarrier i , at time n . The overall CFR for all the subcarriers is shown as,

$$CFR = [CFR(1), CFR(2), \dots, CFR(n)] \quad (20)$$

CFR contains the matrix of $30 \times n$ shows the overall WCI of the different body motions; where n represent the received packets[23]. We present the four body motions and the raw CFR data for these body motions representing the WCI is shown in Figure 7.

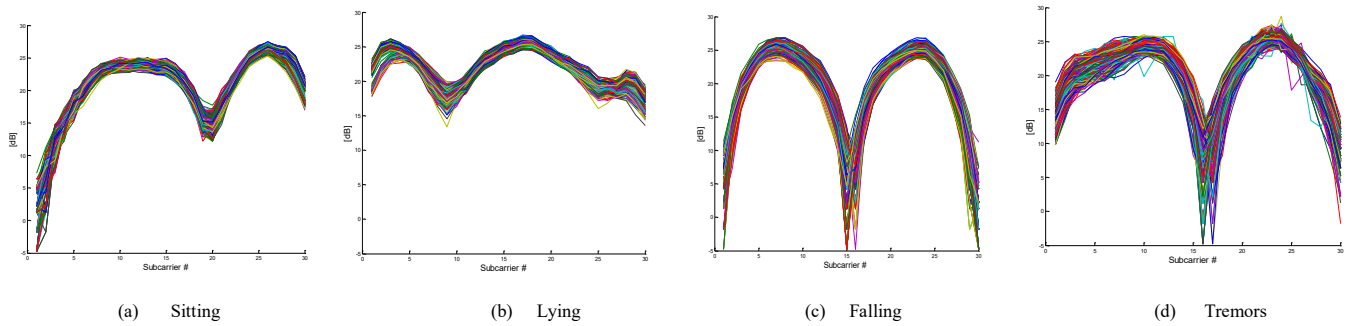


Figure 7: Amplitude history for CFR of different body motions.

The CFR in the Figure 7 shows the changes in the amplitudes for all 30 subcarriers. Different body gestures like sitting, lying, falling due to cramp, and tremors shows different CFR. To clearly observe these changes we choose the sub-carrier number fifteen. The variation in time and amplitude becomes easy to monitor by choosing the sub-carrier number fifteen. The selection of using sub-carrier # 15 [26] depends upon the unique signatures for all of the four body movement rather than other sub-carriers. This gives us more clear and precise information about the time and amplitude of different body movements. This particular choice is very obvious to examine the maximum changes in the CFR of different body gestures.

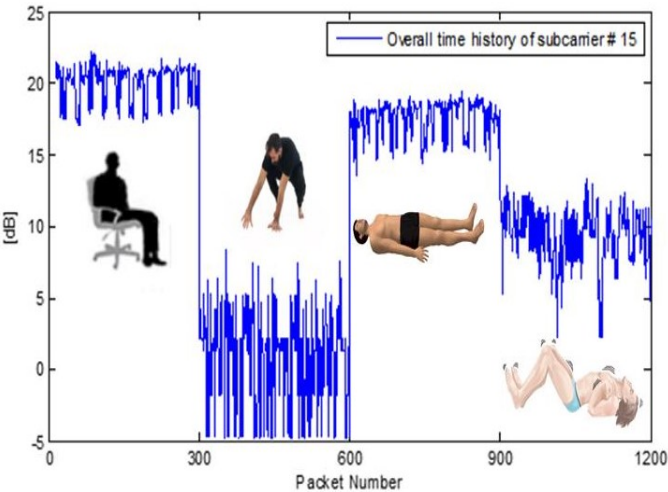


Figure 8: CFR of four different body gestures.

The CFR for four body motions is shown in Figure 8 with the 1200 number of data packets. Every single body motion is represented by total 300 packets of data and the subject stayed for two minutes in each position. There exist many obstacles and multipath components, which considered as the part of the system and the WCI is extracted by keeping in mind about these multipaths as occurred due to scattering, reflection and diffraction. From Figure 8, after careful analysis we can see that the power level for falling and tremors somehow overlap and makes it difficult to differentiate between two body movements. The SVM classifier played important role in that by classifying the data into its particular class and hence the difference becomes easily observable. We also used KNN and RF classifiers along with SVM.

6.1.1 Classification Results using SVM

In this work for the training of the SVM, *svmtrain* (built-in-Matlab function) is used, which works on *one-versus-rest* approach for each of the given class. The sequential minimal optimization (SMO) was performed to set the decision boundary. SVM classifier was trained using two sets of features, for one set 5 time domain features and for second combine 10 time domain features were used. As mentioned earlier each class contains 300 samples of data, out of which 200 samples were used for training and 100 samples for the testing of SVM in each class. We used Polynomial, linear and radial basis function (RBF) Kernel functions. For the measurement of accuracy we used all 10 time domain features one after other. The Table 2 shows the accuracy rate observed by SVM utilizing different number of features. In Table 2, column # 1 shows the types of Kernel functions used for training of the available data sets. The remaining columns show the sitting, lying, falling and tremors represented by C1, C2, C3 and C4. The accuracy increases with the increase of number of features. The accuracy increases as we move towards the polynomial and RBF but SVM shows less accuracy with linear Kernel function. As shown in Table 2,

--	--	--

Kernel Function	5 Features				10 Features			
	C1	C2	C3	C4	C1	C2	C3	C4
Linear	92.75	98.00	100	89.50	93.75	98.00	100	91.25
Polynomial	96.75	97.50	100	93.25	96.75	99.75	100	95.75
RBF	96.00	98.00	100	93.75	95.75	98.25	100	96.60

Table 2: SVM accuracy rate for each class.

In this work, the SVM is using 10 time domain features and 300 total samples for training and testing of SVM for every single class. Out of the four classes, those which are normal show positive values for the training of data samples and the rest show negative or false values. To observe the SVM performance we must select the reasonable number of features for the extraction of desired information from the available classes. Cross validation shows the reliability of any algorithm and needs to be performed for precise results. In our work for the training of SVM we used 5-fold cross validation. The main expression for that is shown as,

$$CV_{(k)} = \frac{1}{k} \sum_{i=1}^k Err_i \quad (21)$$

Err_i represents the number of misclassifications of the i^{th} model on the i^{th} test set.

We can calculate the misclassification rate for all of the four classes by utilizing the three mentioned kernel functions. This misclassification rate shows us the feasibility of using polynomial and RBF kernel functions. Linear always gives more misclassification rate. As shown in Table 3.

Kernel Function	5 Features				10 Features			
	C1	C2	C3	C4	C1	C2	C3	C4
Linear	92.75	98.00	100	89.50	93.75	98.00	100	91.25
Polynomial	96.75	97.50	100	93.25	96.75	99.75	100	95.75
RBF	96.00	98.00	100	93.75	95.75	98.25	100	96.60

Table 3: Error rate or misclassification rate for four classes.

Like accuracies the polynomial and RBF show less misclassification rate as compared with linear Kernel function. The three Kernel functions used total 10 time domain statistical feature vectors to classify the data into four classes and showed the accuracies and misclassification rate by using all the 10 feature vectors. These 10 time domain statistical feature

vectors used for the classification purpose in SVM are shown in Table 4. By using these features vectors we measure the accuracy rate and the misclassification rate as already shown in Table 2 & 3.

$Root\ mean\ square\ (Y_{RMS}) = \sqrt{\frac{1}{P} \sum_{i=1}^P x_i^2}$	$Crest\ Factor\ (Y_{CF}) = \frac{\max(x_i)}{Y_{rms}}$
$Marginal\ factor\ (Y_{MF}) = \frac{\max(x_i)}{Y_{SRA}}$	$Skewness\ value\ (Y_{SV}) = \frac{1}{P} \sum_{i=1}^P \left(\frac{[x_i - \mu_x]}{\sigma} \right)^3$
$Square\ root\ of\ amplitude\ (Y_{SRA}) = \left[\frac{1}{P} \sum_{i=1}^P \sqrt{ x_i } \right]^2$	$Impact\ factor\ (Y_{IF}) = \frac{\max(x_i)}{\frac{1}{P} \sum_{i=1}^P x_i }$
$Mean\ value\ (Y_{MV}) = \frac{1}{N} \sum_{i=1}^P x_i$	$Peak\ to\ peak\ value\ (Y_{PPV}) = \max(x_i) - \min(x_i)$
$Kurtosis\ value\ (Y_{KV}) = \frac{1}{P} \sum_{i=1}^P \left(\frac{[x_i - \mu_x]}{\sigma} \right)^4$	$Standard\ deviation\ (Y_{STD}) = \sqrt{\frac{1}{P} \sum_{i=1}^P (x_i - \mu_x)^2}$

Table 4: Features used for SVM.

As shown in the Table 2, if we compare the accuracies from three different kernel functions, polynomial and RBF shows remarkable increase in the accuracies, approximately 3% to 4% as compared with liner. If we look at Figure 8, the CFR of falling and tremors shows greater similarities. So we processed the data by extracting the best possible features to identify and overcome these similarities. We choose best features which showed remarkable and reliable performance. The time domain features [30] were extracted to get reliable information for the motion. In this work we used Fisher's ratio [28] for the screening and selection of features. As the Fisher's ratio increases, the separation between the classes also increases. The formulation of Fisher's ratio is shown as,

$$J = \frac{(\mu_1 - \mu_2)^2}{s_1^2 + s_2^2} \quad (22)$$

Where μ_1 and μ_2 are the means of falling class and tremor class, s_1^2 and s_2^2 are respective variances. For all the candidates features we calculated the Fisher's ratio as shown in Figure 9. The features which showed higher performances were 2, 4, 6, 9, and 10. They showed the higher separability between the classes. Fisher's ratio showed us the best possible features and improved the result of the classifier. The best features are shown in Figure 9.

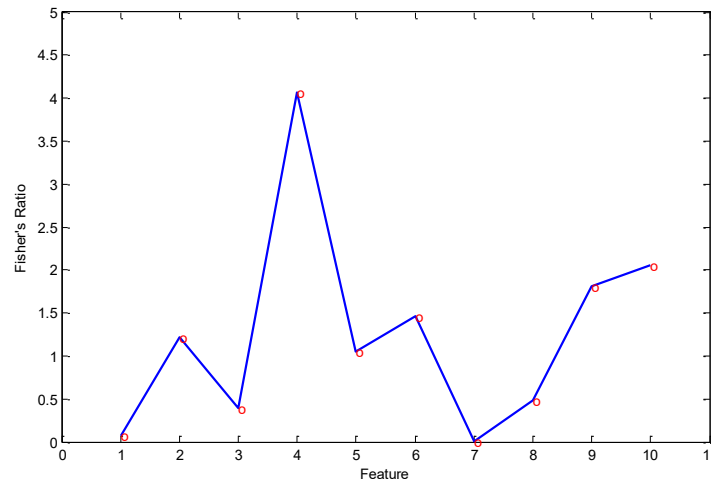


Figure 9: Fisher's Ratio plot for best features.

As mentioned before to show the different actions in a feature space we choose the best features as shown in Figure 9, which are mean μ , standard deviation σ , and the kurtosis. Figure 10 shows the actions of four body motions in their feature space.

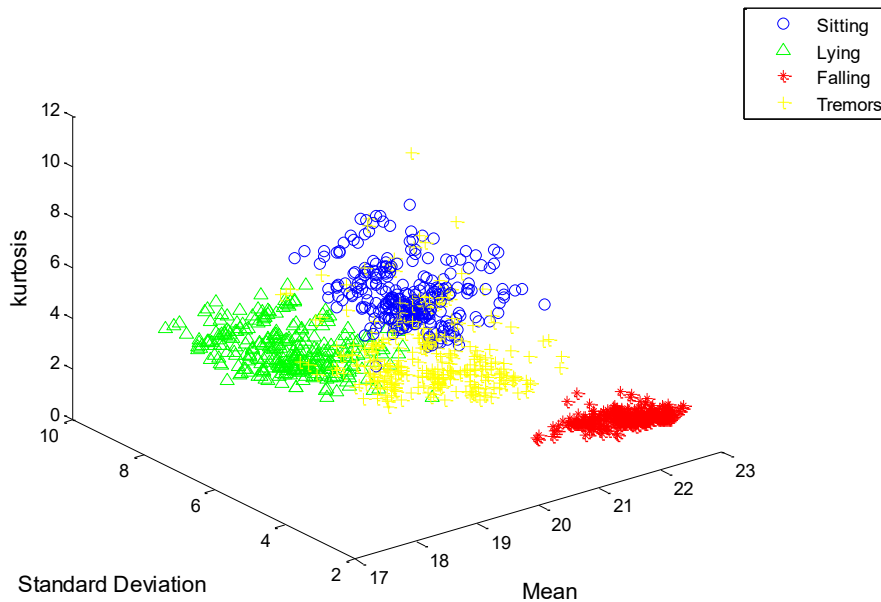


Figure 10: Four body actions in their feature space.

6.1.2 Classification results using KNN and RF

In this section we discussed the classification of C-Band collected data by using the KNN and RF algorithm. Considering the majority votes, all the classes were assigned with the new objects by k nearest object. The training process of KNN algorithm has two parts, first it stores the features and second it allocates the class labels to the available training data-set. There are many distance parameters being used by KNN algorithm as mentioned in the previous equations from (15) to (18). In our research we have utilized the Euclidean distance and adjusted the value for $k = 1$. The RF classifies the data by integrating it into

separate decision trees [34]. A simple tree in the RF classifier holds the M number of leaves and works on feature space by dividing it into M number of regions like $R_n, 1 \leq n \leq M$. Each tree in RF has the prediction function defined as,

$$f(a) = \sum_{n=1}^M c_n \mathfrak{I}(a, R_n) \quad (23)$$

Here the M represents the overall regions in the feature space, R_n represents the n regions, and c_n indicates the constant number that correlates to n . The indicator function is defined by \mathfrak{I} .

$$\mathfrak{I}(a, R_n) = \begin{cases} 1, & \text{if } a \in R_n \\ 0, & \text{otherwise} \end{cases} \quad (24)$$

In RF algorithm the maximum votes from all of the available trees define the final decision function. For our research we used RF classifier by selecting 100 trees.

We used the six performance metrics for examining the classified data using RF and KNN. The performance metrics are precision, accuracy, specificity, recall, F-measure and Cohen's Kappa coefficient.

- i. Precision is defined as the fraction of relevant instances among the retrieve instances [35].

$$Precision = \frac{Tp}{Tp + Fp} \quad (25)$$

- ii. Accuracy is defined as the total number of correct classified instances [36].

$$Accuracy = \frac{Tp + Tn}{Tp + Tn + Fp + Fn} \quad (26)$$

- iii. Recall is the fraction of relevant instances that have been retrieved over the total amount of relevant instances [35].

$$Recall = \frac{Tp}{Tp + Fn} \quad (27)$$

- iv. Specificity measures the proportion of negatives that are correctly identified [37].

$$Specificity = \frac{Tn}{Fp + Tn} \quad (28)$$

- v. Kappais the measure of agreement between the two individuals e.g., simple system and random system [38].

$$Kappa = \frac{(Accuracy - Accuracy_{expected})}{1 - Accuracy_{expected}} \quad (29)$$

- vi. F-measure represents the harmonic mean obtained from sensitivity and accuracy.

$$F - measure = \frac{2Tp}{(2Tp + Fp + Fn)} \quad (30)$$

We used 200 samples for the training of KNN and RF classifier. The confusion matrices we obtained for KNN, RF and SVM classifier are shown in Table 5(a), 5 (b) and 5 (c).

Class (C1,C2,C3,C4)	5 (a)			
	Confusion matrix obtained using SVM for 200 training samples			
	Sitting	Lying	Falling	Tremors
Sitting	191	1	0	4
Lying	2	196	0	2
Falling	3	1	200	1
Tremors	4	2	0	193

Class (C1,C2,C3,C4)	5 (b)			
	Confusion matrix obtained using KNN for 200 training samples			
	Sitting	Lying	Falling	Tremors
Sitting	185	5	0	7
Lying	6	179	1	13
Falling	4	6	196	5
Tremors	5	10	3	175

Class (C1,C2,C3,C4)	5 (c)			
	Confusion matrix obtained using RF for 200 training samples			
	Sitting	Lying	Falling	Tremors
Sitting	189	12	13	10
Lying	6	165	8	3
Falling	3	10	172	6
Tremors	2	13	7	181

Table 5: SVM, KNN and RF classification results.

The above Table 5 shows us the three confusion matrices which we obtained by using SVM, KNN and RF classifier. These confusion matrices give us the clear comparison of SVM, KNN and RF algorithm.

We used these confusion matrices to find out different values for six performance matrices to evaluate the three algorithms. The Table 6 shows the values for six performance matrices which include accuracy, recall, F-measure, Specificity, and Kappa. We have already calculated the percentage accuracy by using 10 SVM time domain features by utilizing three Kernel functions as shown in Table 2. The accuracy which we showed in Table 6 is obtained by using 10 SVM time domain features and RBF Kernel function.

Class (C1,C2,C3,C4)	6 (a)					
	SVM (%) Classification results					
	Accuracy	Recall	Precision	Specificity	F-Measure	Kappa
Sitting	95.5	97.4	97.3	99.1	96.4	0.96
Lying	98	98.1	98	99.3	98	
Falling	100	97.51	97.31	99.1	98.7	
Tremors	96.5	96.9	96.5	97.3	96.9	

Class (C1,C2,C3,C4)	6 (b)					
	KNN (%) Classification results					
	Accuracy	Recall	Precision	Specificity	F-Measure	Kappa
Sitting	92.5	95.3	93.9	97.8	93.2	0.89
Lying	89.5	89.5	89.9	96.5	89.7	
Falling	98	92.3	92.9	97.3	95.4	
Tremors	87.5	87.5	90.7	96.8	89.1	

Class (C1,C2,C3,C4)	6 (c)					
	RF (%) Classification results					
	Accuracy	Recall	Precision	Specificity	F-Measure	Kappa
Sitting	94.5	94.3	85.5	93.7	89.2	0.85
Lying	82.5	82.5	90.6	96.9	86.4	
Falling	86.1	86.2	92.4	96.5	88.2	
Tremors	90.5	90.5	89.2	95.9	89.8	

Table 6: Classification result w.r.t performance matrices.

The Table 6 shows the result of six performance matrices using SVM, KNN and RF algorithm. The accuracy for SVM for sitting is 95% and falling has maximum of 100% accuracy, as also mentioned in Table 2. The recall and precision have almost identical values varybetween 96 % and 98 %. The specificity has the maximum value of 99% and F-measure has 98.7 %. The overall Cohen's Kappa coefficient value for SVM classifier is 0.96 %. The Table 6 also shows the values of six performance matrices using KNN algorithm. The accuracy and recall values for all four human activities vary between 92.5 % and 87.5 %. The sitting has the maximum precision of 93.9 % and lying has the less precision of 89.9 % as compared with all four bodymotions. The maximum value for the specificity reaches up to 97.8 % and F-Measure 95.4 %. For KNN the Cohen's Kappa Coefficient's obtained average value is 0.89 %. For RF algorithm the accuracy values for sitting, lying, falling and Tremors are 94.5 % 82.5 % 86.1 % and 90.5 % respectively. The recall values are almost identical with accuracy. The precision values for sitting and Tremors are less than 90 % and the other two are more than 90 %. The specificity of sitting is 93.7 % and the remaining three values are around 96 %. The average value for Cohen's Kappa coefficient is 0.85 %.

We have compared the results from all six performance matrices for SVM, KNN and RF classifier and concluded that SVM showed more accurate results as compared with KNN and RF. The SVM showed more accuracy and precision almost more than 90 % but the KNN and RF showed fewer values for accuracy. For SVM the average value of Cohen's Kappa coefficient is 0.96 % which is very close to 1 but the KNN and RF values are less. From all this analysis the SVM showed better result.

6.2 Breathing detection

In this section we monitor the chest movement of a patient by extracting the WCI from given setup as shown in Figure 6. The normal and abnormal breathing session of a patient [25] was tracked using invasive digital respiratory sensor (HKH-11C) and WCI from C-band. The devices used for the monitoring of body movement were also used for extracting the WCI for breathing. During the respiratory tracking process the continuous movement of chest moves the signal between LOS and NLOS.

6.2.1 Normal Breathing

We used 5G C-band sensing technique for the extraction of WCI, operating at 4.8GHz. The 5G improved the quality of this technique and future this could be valuable for massive amount of data using the best possible 5G scenarios.

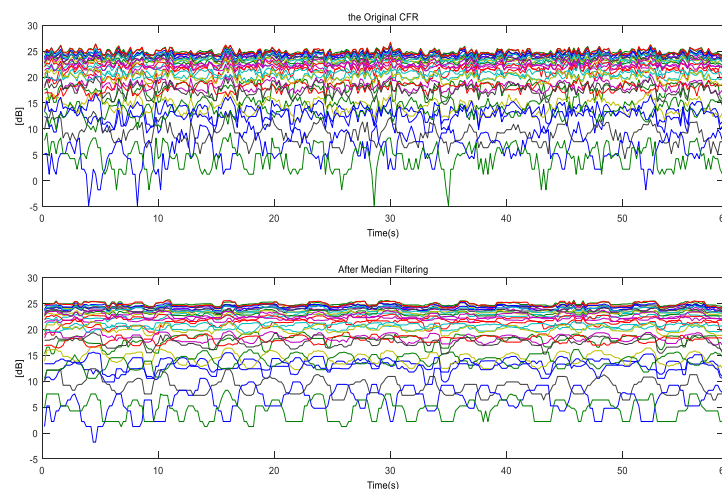


Figure 11: The CFR with all 30 sub-carriers for normal breathing.

The Figure 11 shows the fluctuation in the information regarding amplitude of all the 30 subcarriers with in the period of 60 seconds. All the 30 sub-carriers are clearly visible with different colors in Figure 11. This experiment was performed in a conference room on a volunteer person lying in a straight position for the monitoring of breathing activities. The person imitates the normal and abnormal breathing for the period of 2 minutes and then for the period of 3 minutes. We performed that for couple of times to obtain the precise measurements for the breathing activities. We got the information from all the 30 subcarriers but to extract the exact and refined information we choose the subcarrier number 13 as shown in Figure 12. This shows us the reliable WCI for normal breathing.

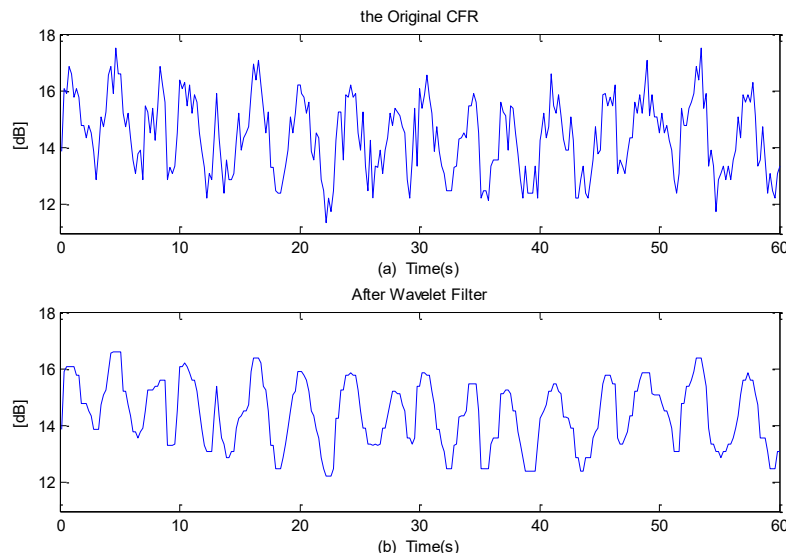


Figure 12: Time history and comparable filtered data using C-Band. (a) Amplitude information for the 13th sub-carrier. (b) Filtered amplitude information using filter.

As shown in the Figure 12(a), we examine the 13th subcarrier which carries the WCI for normal breathing. The amplitude fluctuates as a person inhales and exhales the air and is clearly observable in Figure 12(a). To refine the CFR values, a median filter was used as shown in Figure 12(b). There are many traditional filters available for the suppressing of unwanted noise and fluctuation like Butterworth and Chebyshev etc. But these filters show less convenience while removing the high frequency noise and amplitude fluctuation and also alter the rising and falling edges of the signal. So the obvious choice was the median filter and wavelet filter, which maintains the rising and falling edges and also suppresses the unwanted noise components in the signal.

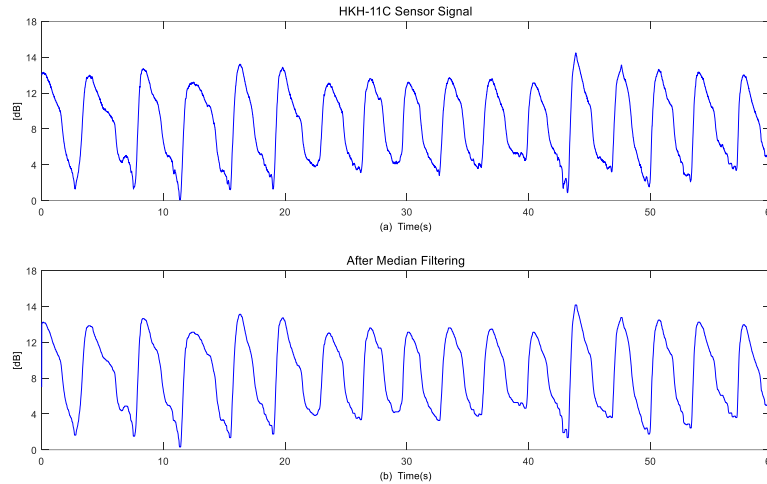


Figure 13: Digital Respiratory sensor information of normal breathing. (a) The normal measured data for normal breathing. (b) The filtered data for normal breathing.

Figure 13 shows the breathing activity observed by digital respiratory sensor and Figure 12 shows the breathing pattern extracted from C-band sensing. Now if we compare the two results from Figure 12(b) and 13(b), the both indicate the approximately 16 breathing cycles during the period of 60 seconds. The CFR from C-band sensing is a bit sensitive due to the external affects like scattering, reflection etc. The breathing sensor data is then compared with the C-band extracted WCI to show the feasibility of using C-band sensing. Matlab was used for the post processing of the extracted WCI data from both sensor and C-band sensing and shows some suitable breathing activities.

6.2.2 Abnormal Breathing

For the monitoring of abnormal breathing we performed the experiment in the same way like normal breathing.

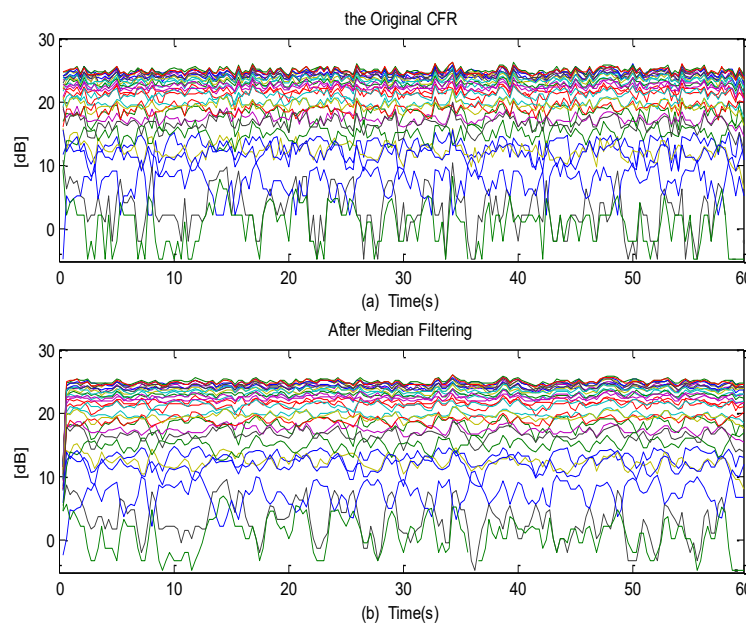


Figure 14: The CFR with all 30 sub-carriers for abnormal breathing.

The raw WCI for abnormal breathing is shown in the Figure 14, contains information of 30 subcarriers for time period of 60 seconds. In this subject was again lying in a straight position and mimic the abnormal breathing during sleep.

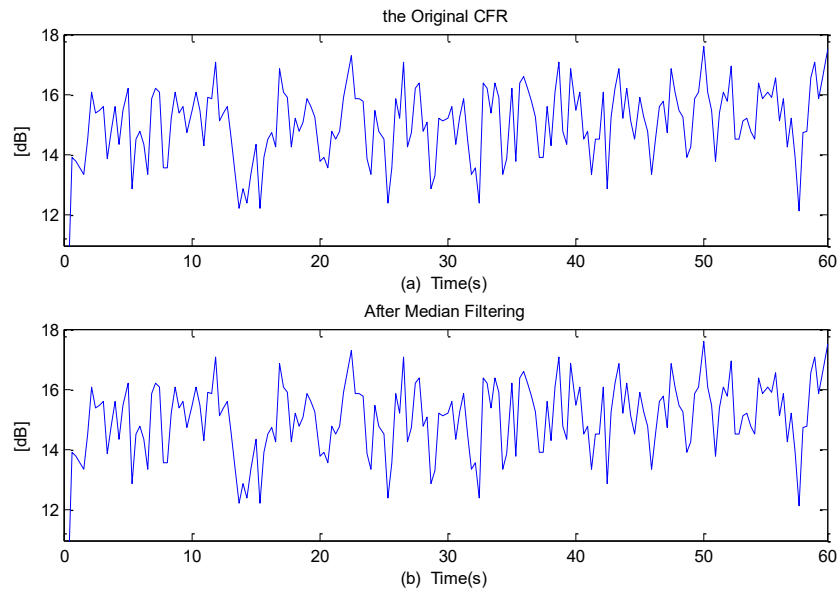


Figure 15: Time history and comparable filtered data using C-Band. (a) Amplitude information for the 16th sub-carrier. (b) Filtered amplitude information using median filter.

The Figure 15 shows the CFR of abnormal breath detection using C-band. The WCI shows more fluctuation in the amplitude as breathing becomes difficult so it disturb the wireless signals travelling from transmitter to receiver. We choose the subcarrier no 16 to clearly observe the difference in amplitude and monitor the abnormal breathing. Digital respiratory sensor data shown in Figure 16 was also compared with the C-band sensing WCI data.

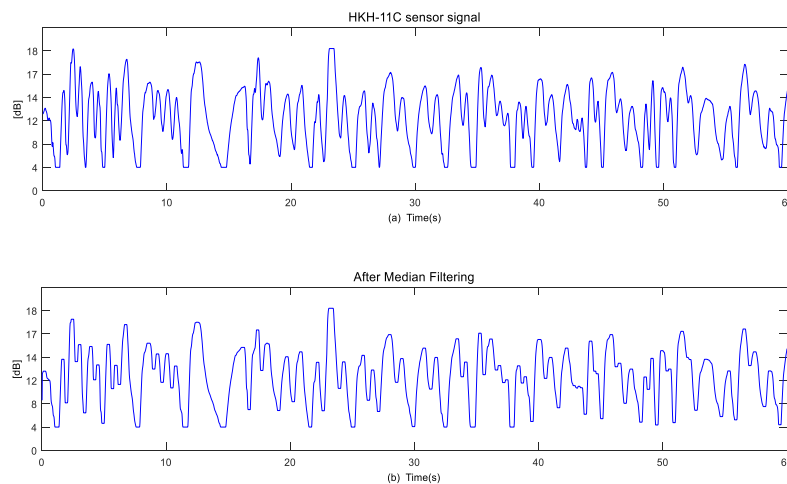


Figure 16: Digital Respiratory sensor information of abnormal breathing. (a) The normal measured data for abnormal breathing. (b) The filtered data for abnormal breathing.

All the subcarriers were tested but the 16th subcarrier shows reliable results for the time period of 60 seconds. Figure 16 shows the sensor data for abnormal breathing. From the Figure 15 we can observe the fluctuation in the amplitude is between 0 to 18 dB which indicates the WCI for abnormal breathing. Here we showed the breathing sensor data just to compare with WCI [39] from C-band and demonstrated that implemented design is the reliable and effective solution for the breathing detection as compared with other wearable devices.

6.3 Spearman's Rank Correlation

In this research we used two sets of data for breathing activity, one from wearable sensor and one from C-Band. We also find the correlation between the two sets of data by using the Spearman's rank correlation. The structure of Spearman's correlation stands on the rank method in which the rank difference gives the information about the correlation coefficients. This rank difference gave us the information about the correlation between two obtained signals. The Spearman's correlation shows quicker computation usually in the presence of limited observations. The Spearman's correlation coefficient has the formula as follows,

$$r_k = 1 - \frac{6 \sum D^2}{N^3 - N} \quad (23)$$

Here the r_k represents the coefficient of rank correlation, D represents the rank differences and N represents the total number of pair observations. The r_k has the value usually lies in between +1 and -1. If the r_k has the positive value than it means the rank has the same direction and if it has negative value, then the rank has the opposite direction. We have used two signals, one from wearable sensor and one from C-Band and we have compared them as shown in Figure 12b and 13b. The r_k value we obtained is 0.88. This shows that the rank has the positive value and very close to 1. We have also compared the waveforms for the abnormal breathing as shown in Figure 15b and 16b. We obtained the value of r_k as 0.87, which is also positive and close to 1 and shows that rank is in the same direction. After the correlation we got a conclusion that the two waveforms we captured from breathing sensor and C-Band are almost identical in both of the cases.

CONCLUSION

This work focused on the monitoring of different body movements for the patient of Multiple Sclerosis and also measured the minute chest movement. The 5G wireless sensing utilized C-band, which used to extract the WCI for the different body movements. The 5G is used to enhance the capabilities of the technique and compensated huge data for the classification. The SVM classifier is used to classify the wireless data into the particular class. In our case, there are four classes representing the four body movements. The breathing activity is monitored using invasive breathing sensor and then compared with the C-band WCI for breathing. We measure the minute chest movement for normal and abnormal breathing and comparison result shows that C-band sensing is more reliable and easy to handle technology for measuring different breathing patterns. The experimental devices used for that research are every low cost and are easily installable.

REFERENCES

- [1] Yanling Zhao, Xinchang Zhang. “New Media Identity Authentication and Traffic Optimization in 5G network”, *IEEE conference on Advanced Information Technology, Electronic and Sutomation Control (IAEAC)*, March 25-26, 2017, Chongqing, China.
- [2] “D1-4-Xu Ying-Emerging Radio Communication Technology and Applications,” article by *State Radio Monitoring Center of China Radio Monitoring Department*.
- [3] Tan Wang, Gen Li, Jiaxin Ding, Qingyu Miao, Jingchun Li and Ying Wang.” 5G spectrum: Is China Ready?” *IEEE communication Magazine*, July 2015.
- [4] Zheng-Wu Lu. “Research about New Media Security Technology Base on Big Data Era”,*2016 IEEE 14th Intl Conference on Dependable, Autonomic and Secure Computing*, (pp: 933 – 936).
- [5] Elaine wong, Elena Grigoreva, Lena Wosinska and Carmen Mas Machuca, “Enhancing the survivability and power savings of 5G transport networks based on DWDM Rings”, *Journal of Optical Community Network/ Vol. 9, No. 9/September 2017*.
- [6] A. Maeder, A. Ali, A. Bedekar, A. F. Cattoni, D. Chandramouli, S. Chandrashekar, L. Du, M. Hesse, C. Sartori, and S. Turtinen, “A scalable and flexible radio access network architecture for fifth generation mobile networks,” *IEEE Commun. Mag.*, vol. 54, no. 1, (pp. 16–23), 2016.
- [7] Atlas: Multiple Sclerosis Resources in the World, World Health Organization, Geneva, Switzerland, 2008.
- [8] H. L. Zwibel, “Contribution of impaired mobility and general symptoms to the burden of multiple sclerosis,” *Adv. Therapy*, vol. 26, (pp. 1043–1057), 2009.
- [9] George E. Tzelepis, F. Dennis McCool, “Respiratory dysfunction in multiple sclerosis”, *Elsevier, Respiratory Medicines*, Vol 109, Issue 6, June 2015, (pp 671-679).
- [10] Cooper CB, Trend PS, Wiles CM. “Severe diaphragm weakness in multiple sclerosis,” *Thorax* 1985; 40:633e4.
- [11] Howard RS, Wiles CM, Hirsch NP, et al, “Respiratory involvement in multiple sclerosis”,*Brain* 1992; 115(Pt 2):479e94.
- [12] Braley TJ, Segal BM, Chervin RD, “Sleep-disordered breathing in multiple sclerosis”, *Neurology* 2012; 79:929e36.
- [13] Barry R. Greene, Stephanie Rutledge, Iain McGurgan, Christopher Mc Guigan, “Assessment and classifiacation of early stage multiple Sclerosis with Inerial Sensors: Comparison against clinical measures of disease state”, *IEEE Journal of Biomedical and Health Informatics*, Vol. 19, No. 4, July 2015.
- [14] Jiaqi Gong, Yanjun Qi, Myla D. Goldman and John Lach, “Causality Analysis of Inertial Body Sensors for Multiple Sclerosis Diagnostic Enhancement”, *IEEE Journal of Biomedical and Health Informatics*, Vol. 20, No. 5, September 2016.
- [15] Patrica Sampson, chris Freeman, Susan Coote, Sara Demain, Peter Feys, Katie Meadmore and Ann-Marie Huges, “Using Functional Electrical Stimulation Mediated by Iterative Learning Control and Robotics to improve Arm Movement for People with Multiple Sclerosis”, *IEEE Transaction on Neural Systems and Rehabilitation engineering*, Vol. 24, No. 2, February 2016.
- [16] Dimitris Kastaniotis, George Economou ,Spiros Fotopoulos, GerasimosKartsakalis and Panagiotis, “Using Kinect for Assessing the state of Multiple Sclerosis”, *IEEE Conference on Wireless Mobile Communication and Healthcare(Mobihealth)*, Nov 2014, Athens, Greece.

- [17] Fei Yu, Arne Bilberg and Egon Stenager, "Wireless medical Sensor Measurement of Fatigue in Patients with Multiple Sclerosis", *IEEE 32nd Annual International conference of EMBS, Buenos Aires, Argentina, August 31-September 4, 2010*.
- [18] M. Gast, 802.11 Wireless Networks: The Definitive Guide. *Sebastopol, CA, USA: O'Reilly Media, Inc., 2005*.
- [19] X. Yang *et al.*, "Monitoring of Patients Suffering from REM Sleep Behavior Disorder," in *IEEE Journal of Electromagnetics, RF and Microwaves in Medicine and Biology*.doi: 10.1109/JERM.2018.2827705
- [20] W. Z. and X. Xue. "Multi-class support vector machine," in Y. Ma and G. Guo (eds), *support Vector Machines Applications, Springer. , 2014, p. pp 23-48*.
- [21] X. Yang *et al.*, "Wandering Pattern Sensing at S-Band," in *IEEE Journal of Biomedical and Health Informatics*.doi: 10.1109/JBHI.2017.2787595
- [22] S. A. Shah *et al.*, "Buried Object Sensing Considering Curved Pipeline," in *IEEE Antennas and Wireless Propagation Letters*, vol. 16, pp. 2771-2775, 2017.doi: 10.1109/LAWP.2017.2745501.
- [23] Anette Forsberg, RPT; Malin Andreasson, RPT; Ylva Nilsagard, RPT. "The Functional Gait Assessment in People with Multiple Sclerosis, Validity and Sensitivity to change", *International Journal of MS Care, March/April 2017, Vol. 19, No. 2, pp. 66-72*.
- [24] X. Liu, J. Cao, S. Tang and J. Wen, "Wi-Sleep: Contactless Sleep Monitoring Via WiFi Signals," *Real-Time Symposium (RTSS), 2014 IEEE, Rome, (pp. 346-355)*.
- [25] D. C. Mack *et al.*, "Development and preliminary validation of heart rate and breathing rate detection using a passive, ballistocardiography-based sleep monitoring system," *IEEE Trans. Inf. Technol. Biomed.*, vol. 13, no. 1, pp. 111-120, Jan. 2009.
- [26] S. A. Shah *et al.*, "Posture Recognition to Prevent Bedsores for Multiple Patients Using Leaking Coaxial Cable," in *IEEE Access*, vol. 4, pp. 8065-8072, 2016.doi:10.1109/ACCESS.2016.2628048.
- [27] B. Dong *et al.*, "Monitoring of atopic dermatitis using leaky coaxial cable," in *Healthcare Technology Letters*, vol. 4, no. 6, pp. 244-248, 12 2017.doi: 10.1049/htl.2017.0021
- [28] Shao, Chenhui, *et al.* "Tool wear monitoring for ultrasonic metal welding of lithium-ion batteries." *Journal of Manufacturing Science and Engineering* 138.5 (2016): 051005.
- [29] Ericsson White Paper, Uen 284-23-3204, April 2016.
- [30] Tian, Jing, *et al.* "Motor bearing fault detection using spectral kurtosis-based feature extraction coupled with K-nearest neighbor distance analysis." *IEEE Transactions on Industrial Electronics* 63.3 (2016): 1793-1803.
- [31] B. Sreejith, a. K. Verma, and a. Srividya, "Fault diagnosis of rolling element bearing using time-domain features and neural networks," 2008 IEEE Reg. 10 Third Int. Conf. Ind. Inf. Syst., no. 1, pp. 1-6, 2008.
- [32] H. Phan, M. Maaß, R. Mazur and A. Mertins, "Random Regression Forests for Acoustic Event Detection and Classification," in *IEEE/ACM Transactions on Audio, Speech, and Language Processing*, vol. 23, no. 1, pp. 20-31, Jan. 2015.
- [33] L. Breiman, J. H. Friedman, C. J. Stone, and R. A. Olshen, "Classification and Regression Trees". Boca Raton: CRC Press, 1998.
- [34] L. Breiman, "Random forests," *Journal of Machine Learning*, vol. 45, pp. 5-32, 2001.
- [35] https://en.wikipedia.org/wiki/Precision_and_recall.

- [36] P. S. Kumar and S. Pranavi, "Performance analysis of machine learning algorithms on diabetes dataset using big data analytics," *2017 International Conference on Infocom Technologies and Unmanned Systems (Trends and Future Directions) (ICTUS)*, Dubai, 2017, pp. 508-513.doi: 10.1109/ICTUS.2017.8286062
- [37] https://en.wikipedia.org/wiki/Sensitivity_and_specificity.
- [38] <http://www.pmean.com/definitions/kappa.htm>.
- [39] Z. Yang, Z. Zhou, and Y. Liu, "From RSSI to CSI: Indoor localization via channel response," *ACM Computer. Survey*. vol. 46, no. 2, Nov. 2013, Article no. 25.